Zeitschrift: Schweizerische mineralogische und petrographische Mitteilungen = Bulletin suisse de minéralogie et pétrographie

Band: 82 (2002)

Heft: 2: Diagenesis and Low-Grade Metamorphism

Artikel: Correlation of fluid inclusion temperatures with illite "crystallinity" data and clay mineral chemistry in sedimentary rocks from the external part of the Central Alps

Autor: Mullis, Josef / Rahn, Meinert K. / Schwer, Peter

DOI: https://doi.org/10.5169/seals-62368

Nutzungsbedingungen

Die ETH-Bibliothek ist die Anbieterin der digitalisierten Zeitschriften auf E-Periodica. Sie besitzt keine Urheberrechte an den Zeitschriften und ist nicht verantwortlich für deren Inhalte. Die Rechte liegen in der Regel bei den Herausgebern beziehungsweise den externen Rechteinhabern. Das Veröffentlichen von Bildern in Print- und Online-Publikationen sowie auf Social Media-Kanälen oder Webseiten ist nur mit vorheriger Genehmigung der Rechteinhaber erlaubt. Mehr erfahren

Conditions d'utilisation

L'ETH Library est le fournisseur des revues numérisées. Elle ne détient aucun droit d'auteur sur les revues et n'est pas responsable de leur contenu. En règle générale, les droits sont détenus par les éditeurs ou les détenteurs de droits externes. La reproduction d'images dans des publications imprimées ou en ligne ainsi que sur des canaux de médias sociaux ou des sites web n'est autorisée qu'avec l'accord préalable des détenteurs des droits. En savoir plus

Terms of use

The ETH Library is the provider of the digitised journals. It does not own any copyrights to the journals and is not responsible for their content. The rights usually lie with the publishers or the external rights holders. Publishing images in print and online publications, as well as on social media channels or websites, is only permitted with the prior consent of the rights holders. Find out more

Download PDF: 25.08.2025

ETH-Bibliothek Zürich, E-Periodica, https://www.e-periodica.ch

SCHWEIZ. MINERAL. PETROGR. MITT. 82, 325–340, 2002

Correlation of fluid inclusion temperatures with illite "crystallinity" data and clay mineral chemistry in sedimentary rocks from the external part of the Central Alps

by *Josef Mullis*[1], *Meinert K. Rahn*[2,*], *Peter Schwer*[3], *Christian de Capitani*[1], *Willem B. Stern*[1] and *Martin Frey*[1] *(deceased)*

Abstract

A data set of 71 samples from 42 localities within the external part of the Central Alps is used to compare illite "crystallinity" (IC) and deconvolution fitted peak parameters with fluid inclusion homogenization temperatures from fibre quartz. Fluid inclusions are filled with methane-bearing fluid and were trapped within a temperature range of 200–270 °C. For the majority of localities, carbonate-rich samples show lower IC values than the clay-rich samples, due to retardation of illite crystal growth by early cementation and conservation of the primary, detrital clay fraction. A small number of localities, however, indicate the opposite trend; these are characterized by high ratios of dolomite versus clay minerals in the carbonate-rich sample. Based on chemical and mineralogical data for the clay fraction, we conclude that the presence of dolomite in these samples implies early diagenetic precipitation of salts in semi-arid to arid climates, triggering the formation of early Na-rich smectite.

All deconvoluted phases (chlorite, smectitic phase, illitic-muscovitic phase) show simple trends in their full-width-at-half-maximum and peak position versus fluid inclusion homogenization temperature. A major control on illite "crystallinity" is the amount of the smectitic phase, which varies from 35 to 82%. However, even if the amount of smectitic phase is considered as an independent variable besides temperature, the correlation with illite "crystallinity" is weak and underlines the only semiquantitative character of illite "crystallinity" as a thermal indicator. The clay fraction compositional evolution shows that anchizonal "illites" contain more K, but less Na than their diagenetic counterparts. For K an external source, probably K-feldspar, has to be assumed. From the data set, a temperature of 240 ± 15 °C is derived for the boundary between diagenesis and anchizone (IC = 0.42 Δ°2θ), which is distinctly higher than so far assumed in the literature.

Keywords: Central Alps, fluid inclusion temperatures, illite crystallinity, deconvolution, diagenesis, anchizone, dolomite.

Introduction

Illite "crystallinity" has been widely used to determine the metamorphic grade in subgreenschist facies pelitic rocks (FREY, 1987). The term "crystallinity" refers to the observed width at half height of the 10 Å reflection (KÜBLER, 1967). However, this width at half height is based not only on the status of an illitic structure, i.e. the X-ray scattering domain size of a K-deficient mica structure, but also on the presence of other mineral phases, such as smectites, the stacking order between illitic and smectitic layers (e.g. LANSON and CHAMPION, 1991), and the reaction progress towards equilibrium (MERRIMAN and PEACOR, 1999). Therefore, the crystal growth process is not simply the result of a rearrangement of the structure of a single phase with temperature, but depends also on other factors, such as the initial detrital substratum, the supply of cations by migrating fluids, the structural evolution of the host rock, and the kinetics of crystal growth (FREY,

[1] Mineralogisch-Petrographisches Institut, Universität Basel, Bernoullistrasse 30, CH-4056 Basel, Switzerland. <josef.mullis@unibas.ch>
[2] Institut für Mineralogie Petrologie und Geochemie, Albert-Ludwigs-Universität, Albertstrasse 23b, D-79104 Freiburg, Germany.
[*] Present address: HSK, CH-5232 Villigen, Switzerland.
[3] Eichrainweg 6b, CH-6410 Goldau.

1987). The term "crystallinity" is used here as representing the sum of all factors, including the increase in compositional homogeneity, the decrease in interlayered swelling components, and the advancing perfection of the illite crystal structure (JABOYEDOFF et al., 2001). While a large number of studies describe the transition from smectite to illite qualitatively (e.g. ROBINSON and SANTANA DE ZAMORA, 1999; BAULUZ et al., 2000), little systematic work has been devoted to the various limiting conditions of evolution.

This study from the external part of the Central Alps presents a correlation between illite "crystallinity" values and fluid inclusion homogenization temperatures, the latter of which are taken as a close approximation of the maximum temperatures reached during Neoalpine burial. Rock samples were collected from localities with fluid inclusion homogenization temperatures between 200 and 270 °C. A detailed evaluation of the illite "crystallinity" as an indicator of incipient metamorphism was done by application of a deconvolution fitting procedure to the X-ray diffraction pattern.

Geology and sampling strategy

The Helvetic belt represents a stack of sedimentary nappes that evolved during the Mesozoic and early Tertiary at the northern border of the Tethys Ocean, between the Eurasian and Apulian plates. The northward movement of the African plate, passively pushing the Apulian microplate, led to a closure of the Tethys beginning in mid Cretaceous, and to a continent-continent collision in the Eocene. This terminated sedimentation in the Helvetic belt and started nappe formation from S to N. Burial under tectonic units of more southern origin is documented today by the presence of Penninic and Austroapline klippen on top of the Helvetic nappe stack. This burial led to a diagenetic to lowermost greenschist facies overprint increasing in grade from N to S.

The metamorphic gradient within the Helvetic belt has been documented along several profiles in the Central Alps (e.g. FREY et al., 1980; BREITSCHMID, 1982; RAHN et al., 1995), with the help of extended data sets on illite "crystallinity" (e.g. WANG et al., 1996; FERREIRO-MÄHLMANN,

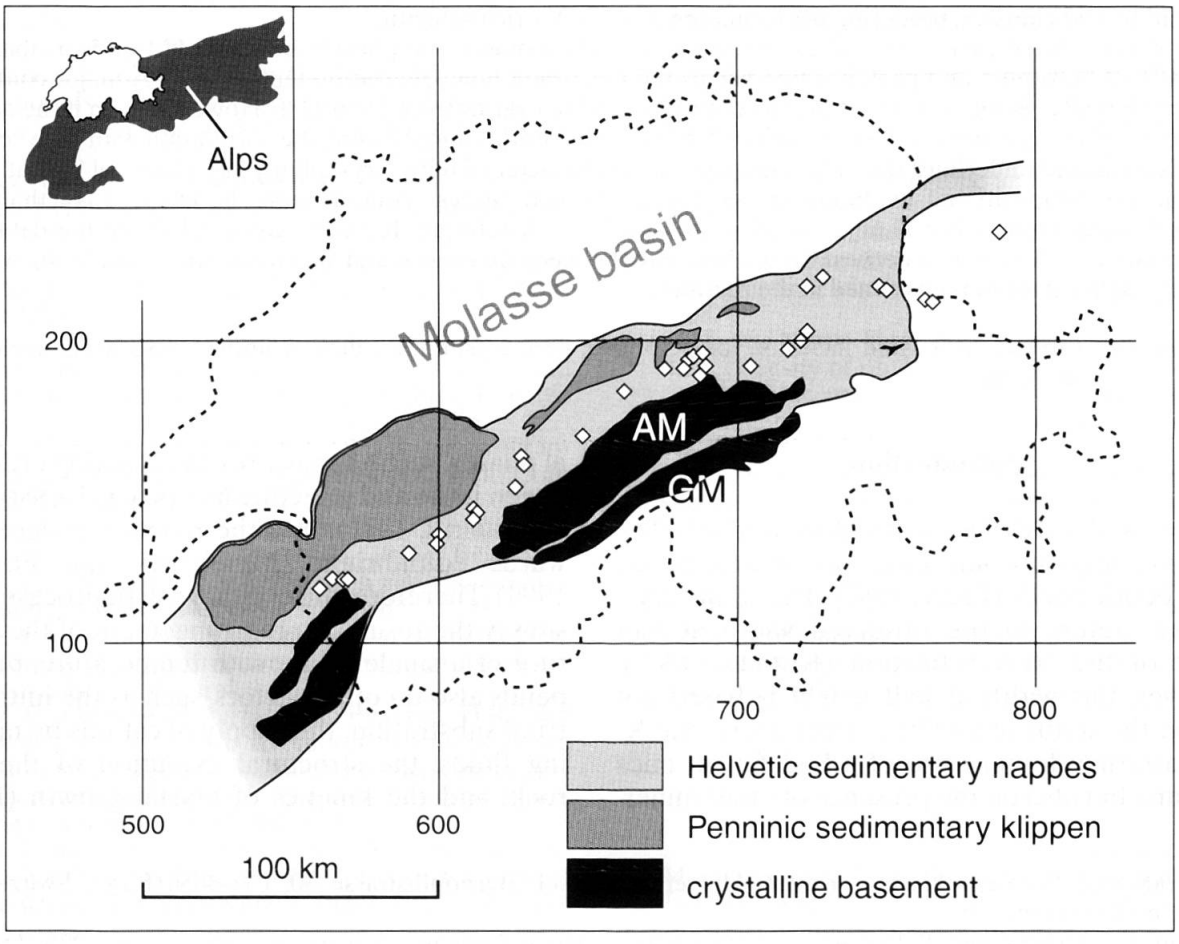

Fig. 1 Sample localities in the northern parts of the Central Alps. For various localities, multiple samples of varying carbonate contents were taken. Coordinates correspond to Swiss map grid (1 unit = 1 km). AM — Aar massif, GM — Gotthard massif.

1995, 1996), vitrinite reflectance (ERDELBROCK, 1994; FERREIRO-MÄHLMANN, 1994, 1995, 1996), and fluid inclusion homogenization temperatures (MULLIS, 1979, 1987). In addition to the classic division into a diagenetic, anchizonal and epizonal belt, the combined applications resulted in a correlation of different methods, and led to the definition of several subzones within the diagenetic and anchizonal realm (e.g. FERREIRO-MÄHLMANN, 1996). In addition to this zonation, other regional divisions were proposed, in particular three fluid zones (MULLIS, 1979, 1987), based on characteristic fluid inclusion compositions: Higher hydrocarbon-rich fluids dominate in the north, methane-dominated fluids are characteristic for the intermediate zone, and methane-depleted water-rich fluids are found in the south. All samples for this study were taken from the methane zone, with maximum homogenization temperatures between 200 and 270 °C, as measured within syn-kinematically grown fissure quartz (Fig. 1). Fluid inclusion homogenization temperatures are interpreted as approximate formation temperatures on the basis of the following arguments: (a) structural field evidences: the boundary between the methane and the water zone crosscuts internal folds in the Helvetic nappes and is itself cut by younger thrust faults (e.g. BREITSCHMID, 1982, MULLIS et al., 1994); (b) fluid inclusion petrography: fluid inclusions that formed during prograde conditions display stretching or decrepitation features, whereas undeformed fluid inclusions were formed during and after peak temperature conditions (MULLIS, 1997); and (c) measured homogenization temperatures of the earliest non-stretched or non-decrepitated fluid inclusions always yield the highest values in all investigated Alpine fissures (MULLIS, 1979, 1987). The samples chosen for this study all fulfill strict requirements for inclusion formation close to peak conditions of diagenesis or metamorphism. For all samples the geologic context suggests similar P-T paths, thus excludes large differences between fluid inclusion and illite "crystallinity" data due to the fact that the former method represents a snapshot of physical conditions during the moment of fluid entrapment, while the latter is thought to be the result of reaction progress and crystal growth during the entire diagenetic/metamorphic evolution.

At several localities, two or three samples were taken within a distance of a few metres, but with large variation in carbonate content. Such a set typically includes a sample of minimum of carbonate component (shale, sample number A, Table 1), a marl of intermediate carbonate content (B), and a carbonate-rich marl to marly limestone (C). With increasing content in carbonate phases (calcite, dolomite), samples commonly lose their schistose appearance.

The data presented originate from 71 samples taken at 42 different localities within the methane zone (MULLIS, 1987) of the Central Alps. Sample localities are displayed in Fig. 1 and listed in Table 1.

Principles and methods

Rock samples were milled and the bulk rock powder measured by XRD for semiquantitative phase determination. After removal of the carbonate phases and application of Atterberg separation techniques, the fraction <2 μm of the samples was sedimented on glass slides with a constant amount of 5 $mgcm^{-2}$. These clay-fraction slides were used for both ED-XRF and XRD analysis. The chemical composition of the <2 μm fraction was measured by ED-XRF using the instrumental equipment and procedure described by STERN et al. (1991). All clay fraction samples were analyzed using a Siemens D-500 diffractometer (Cu-Kα radiation, 40 kV, 30 mA, automatic divergence slits, secondary graphite monochromator).

XRD measurement procedures for deconvolution and classic illite "crystallinity" determination are described in detail in STERN et al. (1991), and satisfy the requirements proposed by KISCH (1991). The full-width-at-half-maximum (FWHM) of the unresolved 10Å complex was determined online after background subtraction, and measured values were corrected against an internal standard (epizonal rock chip). This was followed by mathematical deconvolution fitting of overlapping peaks. The range of diffraction angles chosen for deconvolution varied between 4–11 °2θ (three peaks) in cases where, after background subtraction, no zero level was reached between the first chlorite reflection and the illite-smectite peak complex, and 7–11 °2θ (two peaks) in those cases, where the first chlorite peak was completely separated from the illite-smectite complex.

The deconvolution procedure depends on a number of important conditions and assumptions, which have a distinct influence on the results. Without detailed discussion, which is found elsewhere (e.g. LANSON and CHAMPION, 1991; LANSON and BESSON, 1992; LANSON and VELDE, 1992; STERN et al., 1991), the most important assumptions applied in this study are as follows:

(1) All X-ray reflections derived from single mineral phases are assumed to be symmetric (LANSON and CHAMPION, 1991). The variation in tailing of the illite peak during diagenesis and within the anchizone (as defined by KÜBLER et al.,

Table 1 XRD raw file and deconvolution fitted data (CuK_α radiation) and XRF compositional data for samples from the "methane zone" in northern parts of the Central Alps. FWHM = full width at half maximum, IC = illite "crystallinity" as defined by KÜBLER et al. (1979). IC values are given with three digits, though the significance of the third digit may be questionable.

Sample no.	locality	Swiss map coordinates		T_{hom}	FWHM (Δ°2θ)	FWHM (Δ°2θ)	illitic-muscovitic phase			smectitic phase			chlorite			XRF chemical composition		
		horizontal	vertical	(°C)	air-dried (=IC)	glycolated	FWHM (Δ°2θ)	d-value (Å)	XRD peak area	FWHM (Δ°2θ)	d-value (Å)	XRD peak area	FWHM (Δ°2θ)	d-value (Å)	XRD peak area	K_2O wt%	Na_2O wt%	MgO wt%
Mu-003	Rengglipass	627.560	162.040	223	1.926	0.974	0.516	10.097	62	1.429	10.974	303	0.507	14.129	59	3.51	0.52	5.12
Mu-003A				223	1.767	1.118	0.430	10.040	94	1.803	11.111	510	0.384	14.129	33	4.35	0.65	2.23
Mu-003C				223	1.994	1.048	0.637	9.983	158	1.575	11.182	307	0.412	14.129	37	4.23	0.88	2.06
Mu-010A1	Bundstock S	625.045	151.380	267	0.362	0.393	0.251	10.009	154	0.518	10.267	203	0.311	14.175	52	6.44	0.32	2.41
Mu-010B				267	0.299	0.341	0.214	10.015	100	0.496	10.250	135	0.290	14.216	55	6.06	0.11	3.23
Mu-024-1	First	647.250	168.250	247	0.616	0.526	0.346	10.040	140	0.702	10.394	203	0.249	14.129	19	4.10	0.24	1.00
Mu-024-1A				247	0.735	0.711	0.473	9.983	165	1.102	10.517	243	0.387	14.129	29	5.90	0.55	1.06
Mu-031	Isleten	687.920	196.630	210	0.658	0.532	0.396	10.056	64	1.015	10.588	138	0.288	14.177	57	3.96	0.13	7.06
Mu-035	Attinghausen	689.300	192.220	262	0.397	0.378	0.271	10.000	112	0.818	10.401	186	0.385	14.195	44	5.88	0.44	2.95
Mu-035A				262	0.544	0.418	0.292	10.002	126	0.817	10.430	292	0.368	14.158	44	7.38	0.13	2.80
Mu-035B				262	0.418	0.378	0.246	9.955	103	0.680	10.278	212	0.344	14.116	34	6.44	0.50	3.07
Mu-058A	Choex	563.900	120.800	242	0.391	0.398	0.262	9.969	112	0.589	10.257	188	0.224	14.127	46	7.10	0.10	3.16
Mu-058B				242	0.424	0.489	0.339	10.014	129	0.662	10.369	168	0.284	14.197	34	7.55	0.00	3.05
Mu-059A1	Massongez	564.400	121.350	237	0.475	0.463	0.303	9.978	87	0.668	10.308	138	0.319	14.207	43	7.15	0.03	5.01
Mu-059B1				237	0.397	0.391	0.262	9.990	104	0.674	10.318	171	0.259	14.170	54	5.99	0.23	2.89
Mu-061A1	Tour de Duin	567.730	121.420	244	0.440	0.398	0.271	9.985	173	0.656	10.286	295	0.253	14.148	75	6.41	0.05	3.33
Mu-061B				244	0.380	0.437	0.275	9.999	112	0.676	10.318	194	0.321	14.184	65	5.46	0.26	2.86
Mu-062A	Les Monts	569.700	120.900	241	0.429	0.419	0.293	9.999	134	0.762	10.359	209	0.360	14.177	80	5.54	0.32	2.73
Mu-062B1				241	0.440	0.408	0.293	9.995	228	0.694	10.335	343	0.343	14.143	107	6.01	0.25	2.50
Mu-068-1	Sanetschpass	590.000	129.860	228	0.889	0.764	0.526	10.097	528	1.018	10.580	620	0.261	14.129	86	5.66	0.75	2.24
Mu-071A	Tschingelloch	611.750	143.800	216	0.593	0.564	0.404	10.073	31	1.007	10.511	50	0.291	14.275	6	2.31	0.13	1.55
Mu-072	Engstligengrat	612.000	142.900	202	0.824	0.608	0.370	10.040	29	1.016	10.517	97	0.357	14.129	44	2.37	0.15	2.56
Mu-072A				202	0.984	0.764	0.471	10.021	53	1.331	10.576	137	0.393	14.110	18	4.50	0.43	3.64
Mu-072B				202	0.708	0.721	0.434	10.011	70	1.345	10.475	134	0.298	14.152	24	3.73	0.42	3.38
Mu-073A	Tierhörnli	611.720	141.250	230	0.846	0.777	0.571	9.983	117	1.180	10.644	131	0.327	14.129	22	4.36	0.72	4.50
Mu-074A	Betlis	729.450	222.000	197	0.852	0.596	0.414	10.004	82	0.927	10.473	145	0.574	14.156	35	5.62	0.00	3.80
Mu-074B				197	0.709	0.517	0.346	9.962	55	0.906	10.401	105	0.422	14.078	25	4.82	0.20	3.40
Mu-076	Strahlrüfi	747.860	218.080	223	1.053	0.679	0.456	10.064	148	1.169	10.683	389	0.332	14.171	60	6.08	0.21	2.36
Mu-076-4				223	1.110	0.650	0.417	10.078	117	1.135	10.649	309	0.330	14.186	85	4.13	0.09	3.37
Mu-077	Palvris	749.950	217.730	236	1.321	0.893	0.491	10.084	169	1.387	10.777	654	0.350	14.113	68	4.06	0.74	1.70
Mu-077A				236	0.873	0.654	0.417	10.095	78	1.453	10.680	190	0.313	14.209	45	4.02	0.31	5.54
Mu-081	Fontanella	788.320	236.120	203	1.399	0.684	0.502	10.097	144	1.292	10.773	487	1.257	14.017	62	4.46	0.25	1.30
Mu-202A1	Ijes Fürggli	763.770	214.020	227	1.139	0.848	0.508	9.981	93	1.592	10.598	239	1.516	13.683	40	4.37	0.40	2.54
Mu-203A	Ijes Fürggli SW	763.830	213.770	238	0.592	0.705	0.413	9.983	103	1.208	10.517	257	0.636	14.129	32	5.65	0.36	2.72
Mu-204A	Barthümeljoch SW	765.880	213.380	226	0.643	0.529	0.377	9.983	159	1.071	10.394	293	0.414	14.129	58	6.36	0.00	2.46
Mu-204C				226	0.362	0.324	0.265	9.967	30	0.689	10.282	34	0.240	14.107	8	2.24	0.30	1.12

Table 1 (cont.)

Sample no.	locality	Swiss map coordinates		T_{hom}	FWHM (Δ°2θ)	FWHM (Δ°2θ)	illitic-muscovitic phase			smectitic phase			chlorite			XRF chemical composition		
		horizontal	vertical	(°C)	air-dried (=IC)	glycolated	FWHM (Δ°2θ)	d-value (Å)	XRD peak area	FWHM (Δ°2θ)	d-value (Å)	XRD peak area	FWHM (Δ°2θ)	d-value (Å)	XRD peak area	K_2O wt%	Na_2O wt%	MgO wt%
Mu-236A1	Grat-Attinghausen	687.350	189.000	264	0.354	0.333	0.245	10.001	119	0.574	10.283	169	0.305	14.143	69	5.30	0.22	3.01
Mu-236B				264	0.352	0.363	0.233	10.002	86	0.585	10.285	127	0.324	14.175	69	4.45	0.13	3.38
Mu-262A1	Val d'Illiez	559.700	118.160	249	0.466	0.450	0.298	10.005	186	0.640	10.321	283	0.307	14.190	85	7.01	0.01	3.05
Mu-262B				249	0.489	0.439	0.280	9.983	141	0.675	10.333	309	0.281	14.129	67	6.33	0.23	2.39
Mu-271A1	Linthal	717.750	196.800	271	0.319	0.311	0.229	9.962	197	0.534	10.205	256	0.279	14.195	70	7.56	0.02	3.45
Mu-271B				271	0.327	0.393	0.248	9.983	99	0.509	10.273	161	0.255	14.129	41	6.46	0.04	2.35
Mu-548	Rawilpass	599.240	135.750	201	1.511	0.963	0.721	10.214	162	1.338	10.974	390	0.722	14.129	51	4.86	0.34	1.17
Mu-550	Lac de Tseuzier	599.090	132.980	221	0.714	0.623	0.451	10.097	141	0.715	10.644	88	0.231	14.129	12	3.48	0.01	1.35
Mu-585	Bockialp	661.800	183.400	212	2.023	1.056	0.463	10.023	77	1.802	11.132	244	0.315	14.206	24	3.82	0.58	2.20
Mu-587	Klausenpass W	704.430	192.110	211	0.516	0.507	0.334	10.008	297	0.704	10.255	317	0.303	14.116	86	5.58	0.53	1.90
Mu-589	Labria	750.970	216.880	213	1.643	0.964	0.424	10.040	45	1.590	10.974	309	0.338	14.129	23	4.31	0.69	5.09
Mu-606	Schwarzrüfi	748.650	218.840	221	1.532	0.917	0.617	10.214	172	1.131	10.806	483	0.683	13.870	39	4.17	0.66	1.08
Mu-614A	Kleintal-Isenthal	684.630	194.360	202	1.070	0.806	0.492	9.990	135	1.486	10.605	315	0.462	14.072	38	5.41	0.80	1.66
Mu-614-1B				202	0.889	0.832	0.535	10.029	118	1.262	10.600	169	0.382	14.130	13	5.18	0.43	1.91
Mu-620A1	Grosstal-Isenthal	682.080	190.720	234	0.518	0.478	0.336	10.043	216	0.822	10.439	335	0.273	14.220	44	7.45	0.82	2.17
Mu-620B1				234	0.458	0.421	0.348	10.018	131	0.938	10.427	162	0.278	14.158	35	5.53	0.18	3.17
Mu-621A1	Isenthal	685.400	195.650	210	1.252	0.905	0.478	10.078	123	1.366	10.682	557	0.845	13.810	45	5.30	0.40	1.29
Mu-621B				210	1.750	0.850	0.540	10.097	99	1.437	10.773	417	0.664	14.129	67	4.87	0.26	1.74
Mu-622-1A	Kleintal E	685.880	194.670	205	0.716	0.628	0.494	10.018	274	1.453	10.685	330	0.640	14.110	55	4.96	0.48	3.56
Mu-622-1B				205	0.725	0.726	0.552	10.040	130	1.393	10.773	119	0.592	14.243	26	5.36	0.48	1.87
Mu-633A	Bannalp	675.390	190.810	203	0.821	0.824	0.496	10.092	244	0.963	10.579	441	0.313	14.124	28	5.08	0.69	4.23
Mu-633B				203	1.020	0.743	0.500	10.087	181	1.109	10.690	422	0.404	14.104	56	4.80	0.56	3.04
Mu-682A1	Betschwanden	721.430	200.700	256	0.319	0.322	0.225	9.986	157	0.488	10.226	209	0.245	14.149	58	7.33	0.00	2.51
Mu-682B				256	0.322	0.331	0.209	9.943	91	0.522	10.190	155	0.301	14.161	74	5.84	0.00	4.61
Mu-683	Haslen	723.230	204.000	236	0.418	0.380	0.247	9.983	193	0.549	10.273	345	0.284	14.129	75	6.93	0.11	2.78
Mu-684A1	Mollis	724.180	217.940	216	0.708	0.546	0.392	10.029	185	0.953	10.530	374	0.325	14.162	63	6.26	0.02	3.77
Mu-684B1				216	0.518	0.470	0.352	10.000	77	0.876	10.456	116	0.796	14.418	96	4.28	0.00	5.60
Mu-695A	Untere Lattreien	627.780	161.050	225	1.105	0.878	0.502	10.000	79	1.762	10.873	172	0.485	14.101	17	3.67	0.73	1.60
Mu-695B1				225	1.036	0.817	0.599	10.167	99	1.185	10.767	221	0.440	14.176	26	4.09	0.24	1.70
Mu-697A	Glütsch	628.100	159.150	234	0.713	0.654	0.436	10.097	109	1.058	10.580	176	0.509	14.243	8	3.68	0.22	0.81
Mu-697B				234	0.561	0.560	0.424	10.036	43	1.038	10.480	46	0.286	14.227	6	2.04	0.13	1.17
Mu-698A	Bretternhörnli	626.900	159.140	226	0.717	0.643	0.366	10.039	66	0.823	10.454	117	no chlorite		4.090.38	4.08		
Mu-703A	Barthümeljoch W	765.820	213.400	237	0.555	0.647	0.401	9.983	172	1.173	10.455	405	1.044	14.129	36	6.74	0.27	1.48
Mu-704A	Bartümeljoch S	765.770	213.400	237	0.880	0.641	0.431	10.070	83	0.431	10.640	199	0.347	14.166	42	4.23	0.12	2.15
Mu-704B				237	0.432	0.479	0.384	10.041	77	1.204	10.619	62	0.598	14.337	21	3.83	0.64	2.04

1979) is the result of the overlap of at least two reflections. It is not the consequence of a specific apparatus setting (see e.g. KISCH, 1991), as all samples have been measured with the same apparatus. Scattering effects, such as the fanning of mica layers at their grain boundaries (STERN et al., 1991) are minimized or excluded on the basis of a careful handling of the sample during preparation, e.g. by keeping milling times to less than 30 seconds. The assumption of symmetric peaks is in contradiction to results by MOORE and REYNOLDS (1989), which demonstrated increasing tailing of the (001) illite peak with decreasing crystallite size. It is, however, justified in the case of (i) the lack of information about the crystallite size and its evolution with increasing temperature, and (ii) the presence of a clay phase mixture as found in the investigated samples.

(2) X-ray reflections are approximated by Pearson VII functions, which have been shown to provide good fits for both well and poorly crystallized material (STERN et al., 1991).

(3) The d-value of a deconvoluted peak is a *resulting parameter*, and is not derived from a database X-ray pattern. The applied fitting program optimizes peak positions of pre-selected reflections (d-values), but also peak widths, peak areas/intensities and peak shapes in order to obtain a minimum difference between measured and calculated diffraction pattern (expressed as a reliability factor).

(4) As a consequence of assumption (3), the number of peaks between 4 and 11 °2θ is restricted to a maximum of 3. This is the result of the commonly observable "bull head" (STERN et al., 1991) in samples of diagenetic grade, generated by the presence of two narrow peaks (at about 10 and 14 Å) and a wide peak in-between. The peaks considered are chlorite (with its (001) reflection of 14 Å at about 6.3 °2θ, a "smectitic phase", with variable d-value, and an "illitic-muscovitic phase", with a peak close to the standard (002) muscovite reflection, at around 10 Å (8.8 °2θ). Peak positions were calibrated against the position of the first quartz (100) reflection at 20.9 °2θ.

A large number of additional mineral phases may be expected to show a major reflection within or near the mentioned 2θ-range. Their presence, however, was not confirmed in any sample by reflections of higher order. This particularly applies for mineral phases such as corrensite, paragonite, pyrophyllite, and kaolinite. The presence of most of these phases is in any case unlikely due to bulk-rock composition and metamorphic grade of upper diagenetic to lower anchizonal grade. Because of the same argument, the presence of biotite, difficult to recognize by X-ray techniques, can be excluded.

Investigations on fluid inclusions in quartz crystals were made with a Chaixmeca heating and freezing stage, designed to work in the range of –180 to +600 °C (POTY et al., 1976). Sample preparation and measurement techniques are summarized in MULLIS (1979, 1987). Careful inclusion petrography was needed before inclusions were measured by microthermometry. For this study, only such localities were investigated, where fluid inclusion formation occurred close to the two-phase boundary of the methane-bearing water-rich and the water-bearing methane-rich phase. Such conditions were either accomplished within pseudosecondary inclusions of synkinematically grown fibre quartz, or in secondary methane-bearing water-rich fluid inclusions of early prismatic quartz, overgrown by skeletal quartz containing primary water-bearing methane-rich inclusions (MULLIS, 1976, 1979, 1987). The homogenization temperature of the earliest methane-bearing water-rich fluid inclusions (homogenization of the aqueous phase with the methane bubble) occurs in the laboratory at saturation conditions thought to reflect the approximate formation temperature.

Results

Classic illite "crystallinity" values (determined at the 10 Å complex after KÜBLER et al., 1979) for 71 clay fraction samples vary between 0.30 and 2.02 Δ°2θ (Fig. 2). The same sample set yields FWHM values for glycolated samples of 0.32–1.12 Δ°2θ. The obtained "crystallinity" values illustrate that the metamorphic grade from all sample localities varies from diagenetic to medium-grade anchizone, if applying 0.42 and 0.25 Δ°2θ as the anchizone boundaries (KÜBLER et al., 1979). A comparison between air-dried values (illite "crystallinity" sensu stricto), and the glycolated values, indicates the presence of swelling components within the measured clay fraction. With beginning of the anchizone (240 ± 15 °C), there is no longer a visible difference between air-dried and glycolated FWHM values. Within the entire temperature range of 200–270 °C, the difference between air-dried and glycolated, however, decreases from nearly 1.0 Δ°2θ to zero (Fig. 2).

For samples collected at the same locality, a variation in illite "crystallinity" by up to a factor of 2 is observed. This variation in IC values does not show an obvious systematic pattern. In most cases, carbonate-rich samples show smaller IC values than clay-rich samples. There is, however, a small number of samples showing the opposite trend, i.e. higher IC values for carbonate-rich

samples than the clay-rich samples from the same locality. In order to identify the cause for the deviating behaviour, a "dolomite ratio" was defined for the carbonate-rich sample of each locality as the peak intensities of the dolomite (104) main peak (2.89 Å at 31 °2θ) divided by the sum of the illite/smectite and chlorite peak intensities at 6–10 °2θ. It was found that samples with a dolomite ratio > 4 systematically display higher IC values than the clay-rich samples. In contrast, carbonate-rich samples with a dolomite ratio < 4 yield smaller illite "crystallinity" values than the clay-rich samples (Fig. 3).

The comparison between fluid inclusion homogenization temperatures (covering a temperature range from 197 to 271 °C) and illite "crystallinity" (Fig. 2) shows a general trend of decreasing peak widths with increasing fluid inclusion temperature. It is evident that the data are characterized by a large scatter in peak width values in the lower half of the temperature range. Here, illite "crystallinity" values may vary between 0.5 and 2.0 Δ°2θ while glycolated peak widths have a reduced vertical scatter of only 0.5 to 1.1 Δ°2θ.

By deconvolution, a set of four parameters can be obtained, three of which reveal a trend with increasing temperature. Deconvolution data are given as FWHM values (derived from the deconvoluted α_2-corrected peaks) and d-values for each separated phase, for this study called "smectitic" and "illitic-muscovitic" phase. For the smectitic phase, values vary considerably between 0.43 and 1.80 Δ°2θ (FWHM) and between 10.205 and 11.182 Å (d-value). In contrast, for the illitic-muscovitic phase the variation is restricted to values between 0.21 and 0.72 Δ°2θ (FWHM) and between 9.943 and 10.214 Å (d-value). At higher temperatures, all parameters show less scatter and, with exception of the illitic-muscovitic phase, a decrease in d-values (Fig. 4).

A semi-quantitative estimation of the amount of the smectitic phase was achieved by comparing the areas of the deconvoluted smectitic, illitic-muscovitic and chlorite peaks: the smectite content was defined as the area of the smectitic peak divided by the sum of areas of the smectitic, illitic-muscovitic and chlorite peaks. Samples with 35–61% smectitic content tend to show relatively

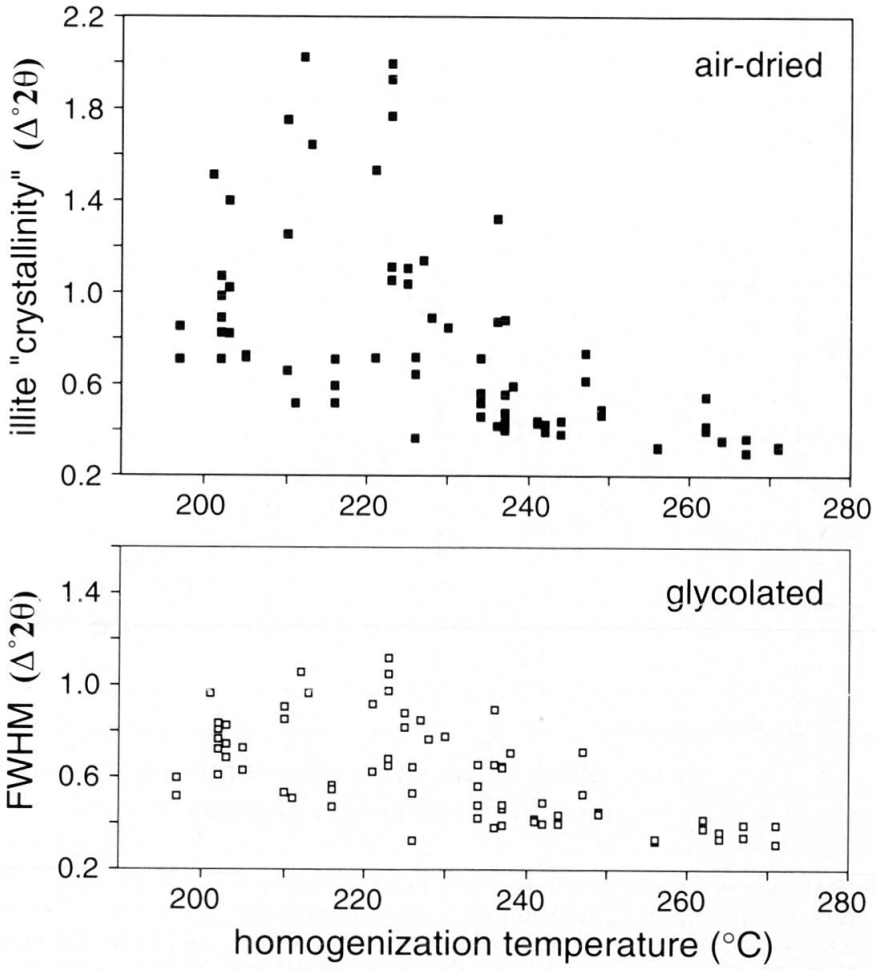

Fig. 2 Measured full width at half maximum (FWHM, unresolved 10 Å complex = illite "crystallinity") for air-dried and glycolated samples versus fluid inclusion homogenization temperature in fibre quartz.

small FWHM values (below 1.2 Δ°2θ, while those with smectitic contents between 62 and 82% show FWHM values of 0.6 to 2.1 Δ°2θ (Fig. 5).

From the XRF chemical analyses of the < 2 μ fraction, a statistical evaluation on chemical influences on illite "crystallinity" was carried out. A significant regression factor for correlation with illite "crystallinity" was found for Na. Because both Na and Mg are important elements in smectite phases, the ratio $Na_2O/(Na_2O+MgO$ was chosen as a measure for the presence of smectite in the clay fraction. This ratio shows a distinct correlation with illite "crystallinity" values when plotted against temperature (Fig. 5). $Na_2O/(Na_2O + MgO)$ ratios > 0.08 largely correspond to samples of high smectite content (62–82%), and these show high illite "crystallinity" values. $Na_2O/(Na_2O+MgO)$ ratios < 0.08 correspond to lower smectite contents (35–61%) and are characterized by lower illite "crystallinity" values. The $Na_2O/(Na_2O + MgO)$ ratio of 0.08 was derived from the applied statistical evaluation and represents a purely empirical value.

The measured K_2O and Na_2O contents of the clay fractions were compared with illite "crystallinity" values and fluid inclusion homogenization temperatures (Fig. 6). While for Na_2O, only a very faint trend with increasing homogenization temperature is observed, the Na_2O contents in the clay fraction clearly decrease with increasing illite

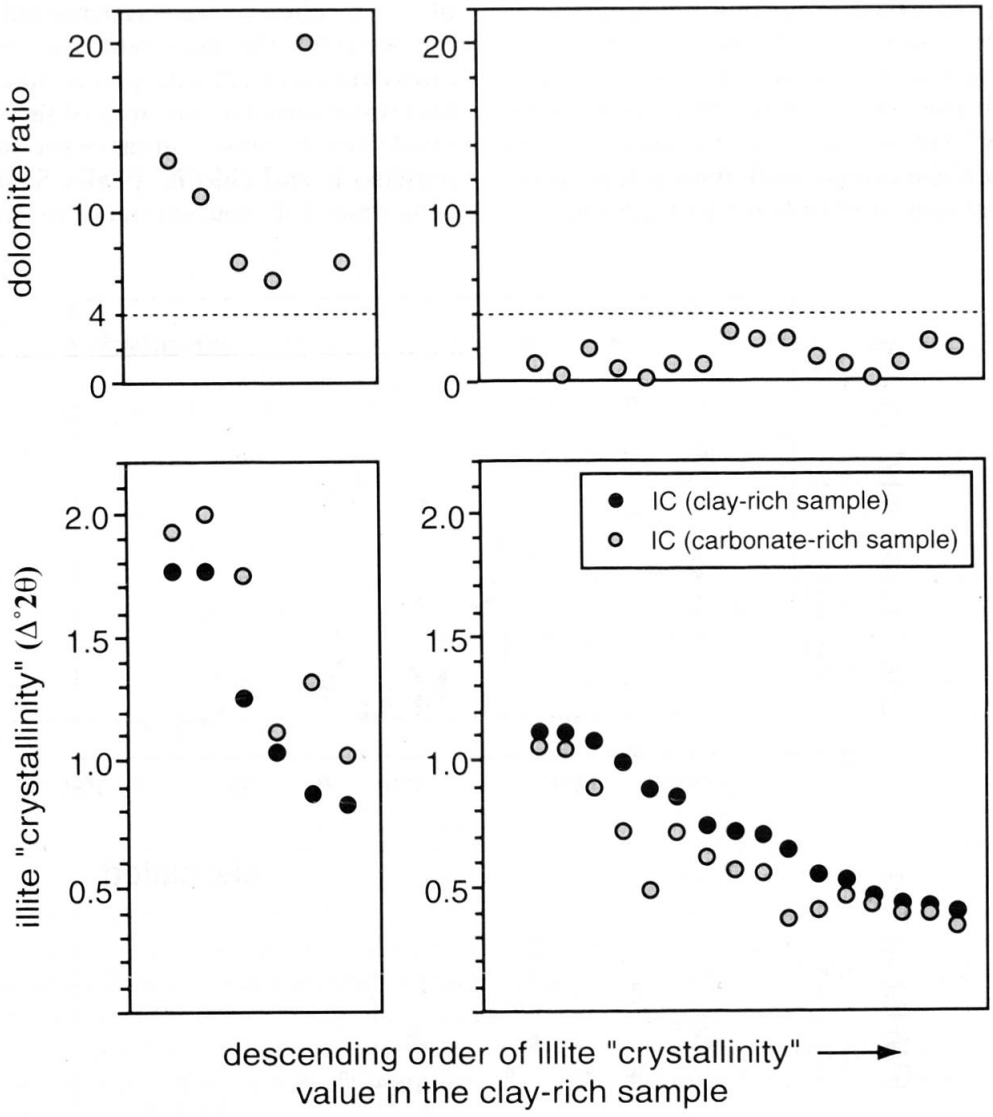

Fig. 3 Diagrams illustrating how illite "crystallinity" depends on the relative carbonate contents and, for carbonate-rich samples, on the relative dolomite contents. Samples are plotted with descending illite "crystallinity" values in the clay-rich sample along the x-axis. Two subgroups are shown, with higher (left) and lower (right) illite "crystallinity" in the carbonate-rich sample. Depending on the dolomite ratio (peak heights of dolomite/sum of clay minerals), carbonate-rich samples with a dolomite ratio > 4 systematically display higher IC values than found for the clay-rich samples. In contrast, carbonate-rich samples with a dolomite ratio < 4 yield smaller IC values than clay-rich samples.

evolution. Trends are even more pronounced for K_2O, which indicates a general increase in the clay fraction with increasing homogenization temperature and a strong increase of K_2O with increasing illite "crystallinity". Similar diagrams for MgO do not show any trends.

Discussion

The assumption that the clay fraction evolves continuously with increasing temperature as an external physical parameter implies that the internal chemical parameters of all investigated samples are constant. Direct comparison of illite "crystallinity" values from different samples as a measure of metamorphic grade is possible only if the clay fractions of the investigated samples have very similar initial chemical and mineralogical composition and the same chemical environment to evolve towards thermodynamic equilibrium. Under such ideal conditions and provided internal and external parameters reached equilibrium, illite "crystallinity" would represent an absolute measure of the integrated thermal history, similar to vitrinite reflectance (e.g. SWEENEY and BURNAM, 1991). Any difference in illite "crystallinity" should then correspond to a difference in physical conditions experienced, of which temperature is thought to be the dominant parameter (FREY, 1987).

In reality, illite "crystallinity" is more likely to be a measure of reaction progress than of the thermodynamic equilibrium reached (ESSENE and PEACOR, 1995). The measured "crystallinity"

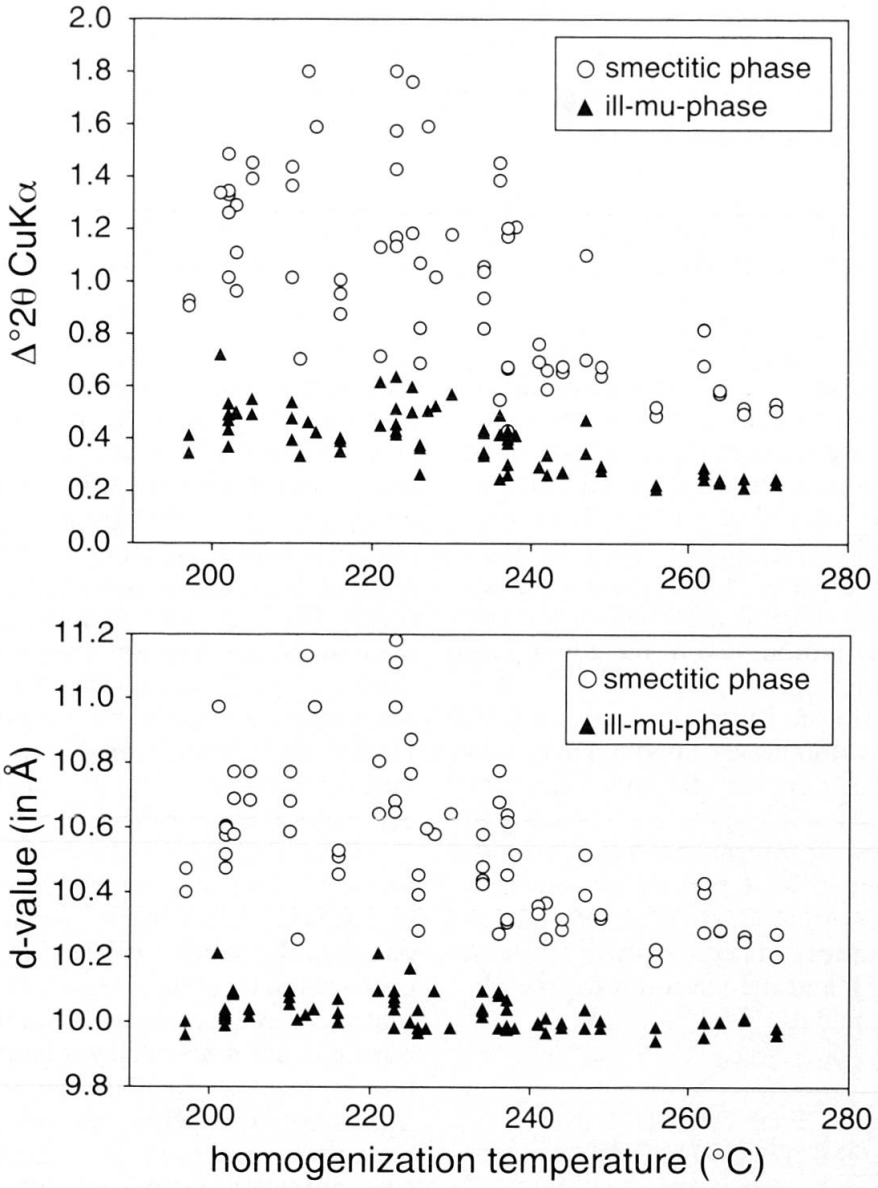

Fig. 4 Evolution of full width at half maximum (FWHM, above) and d-value (below) of the deconvolution fitted smectitic and illitic-muscovitic phase with increasing fluid inclusion homogenization temperature in fibre quartz.

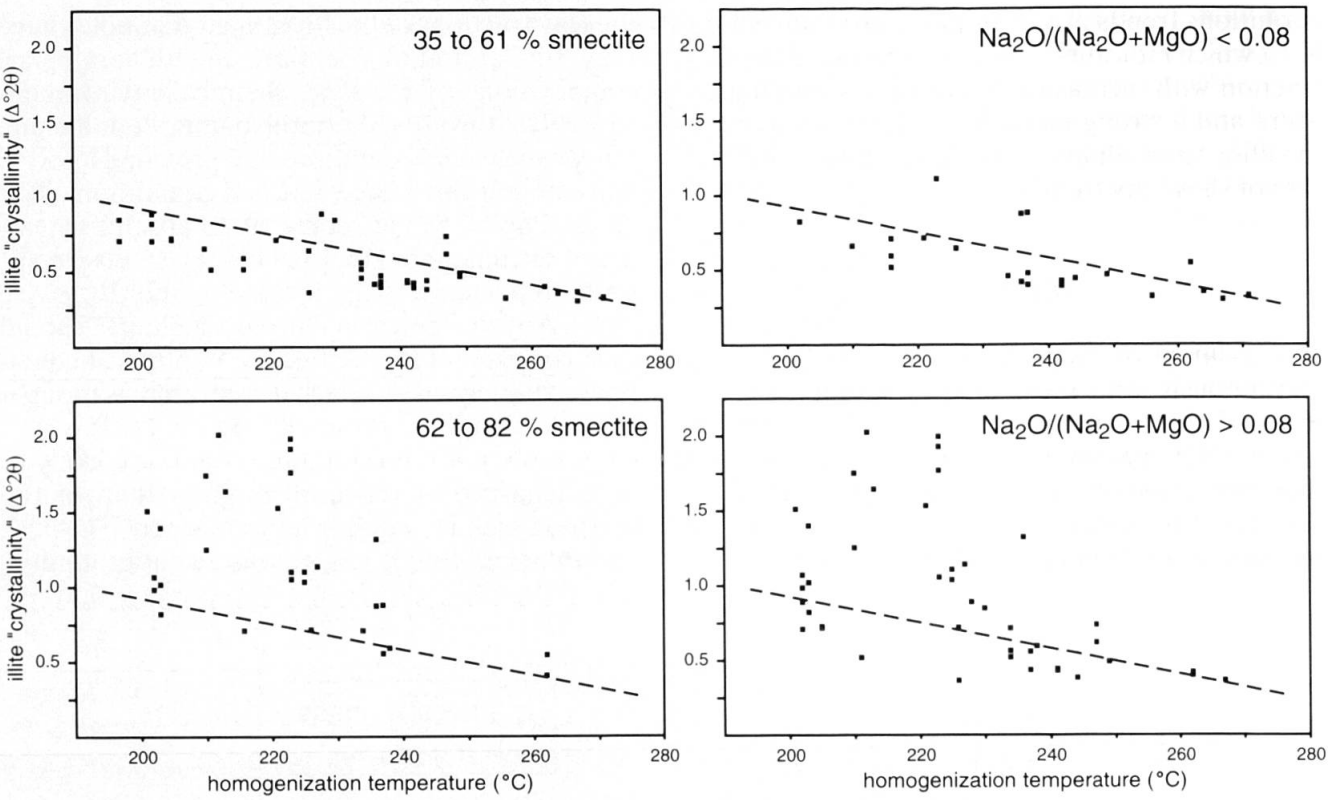

Fig. 5 Relationship between illite "crystallinity" and the smectite content (as defined in the text, diagrams at left) and the clay fraction chemical composition (indicated by the $Na_2O/(Na_2O + MgO)$, as measured on sedimented slides (diagrams at right). For reference only, an arbitrary dashed line is shown; its IC/T_{hom} relationship is the same in all diagrams.

is the result of internal factors, such as composition and crystal size of a detrital clay fraction, and of external factors, such as the supply of nutrients, the structural evolution, as well as physical parameters such as P and T (FREY, 1987; MERRIMAN and PEACOR, 1999). Consequently, illite "crystallinity" is a sensitive parameter of many changes affecting the initial detrital material during the entire thermal evolution, even including late near-surface weathering.

Although the thermal history of the samples investigated in this study is assumed to have been similar, the observed illite "crystallinity" data vary markedly, especially at temperatures below 240 °C. Therefore, a set of internal factors is considered in the following. These factors are shown to have had a distinct influence on illite "crystallinity", i.e. on the kinetics of crystal growth (ESSENE and PEACOR, 1995), and may account for the observed scatter in the data.

THE INFLUENCE OF CALCITE AND DOLOMITE CONTENT

In rocks with little dolomite, illite "crystallinities" are smaller in carbonate-rich rocks than in clay-rich samples from the same locality (Fig. 3). In the carbonate-rich rocks clay minerals suggest a higher grade of reaction progress as deduced from their lower illite "crystallinity" values. A possible interpretation of the observed pattern is the initial presence of a rather immature, but coarse-grained detrital clay fraction in the carbonate-rich rocks. The structural and chemical evolution of the detrital clay fraction was retarded because the fluid in the carbonate-rich rocks was very probably dominated by Ca, but depleted in K and Na. Under these conditions, the clay fraction remained dominated by detrital grains, and did not evolve with temperature.

Elevated relative contents of dolomite (expressed by the dolomite ratio) correlate with larger FWHM values in carbonate-rich rocks compared to the smaller FWHM in clay-rich samples of the same localities (Fig. 3). It may be suggested that the presence of large quantities of dolomite, but small amounts of clay minerals, may have promoted smectite growth by Mg supply. This suggestion is not convincing, because a comparison between Mg content in the < 2 μ fraction and chlorite content (as estimated from the relative peak area) suggests that samples with much Mg also have high chlorite contents, but not necessarily

high smectite contents (Fig. 5). Therefore, the increased Mg supply will primarily have led to chlorite growth. This assumption can be tested by plotting the relative chlorite peak area (i.e. the chlorite peak area divided by the sum of chlorite, smectitic, and illitic-muscovitic phase areas) against the $Na_2O/(Na_2O + MgO)$ parameter (Fig. 7). From this figure, it is deduced that chlorite is the main carrier of Mg in the clay fraction. A more likely explanation for the relation between dolomite content and larger FWHM is as follows: Dolomite is commonly an important early diagenetic cementation phase, found in many sediments deposited in semi-arid to arid climates (TUCKER and WRIGHT, 1990). Such dolomite cements often precipitate from brines and contain salt-rich fluid inclusions (OVERSTOLZ, 2001), which in turn promote smectite growth. The presence of dolomite would thus be but an indicator, and not a direct cause of increased FWHM values. This explanation is supported by the observation that illite "crystallinity" values are large for both carbonate- and clay-rich samples at those localities, where the dolomite ratio is large in carbonate-rich samples (Fig. 3). It appears that early diagenetic cementation and brines affected carbonate-rich rocks as well as the neighbouring shales.

CHEMICAL EVOLUTION OF THE < 2 μ FRACTION

The agreement between the two groups of different smectite contents on one hand, and the different $Na_2O/(Na_2O + MgO)$ ratios on the other (Fig. 5), suggests that most of the smectitic layers present in our samples are Na-bearing. From our data set it cannot be estimated how much Na is incorporated into illite. Paragonite is a common phase reported from clays of anchizonal metamorphic grade (FREY, 1987). All X-ray diffraction patterns, however, were carefully checked for the presence of the paragonite (0010) reflection, but none was found. On the other hand, a comparison between illite "crystallinity" and the K_2O content in the clay fraction (Fig. 6) indicates that anchi-

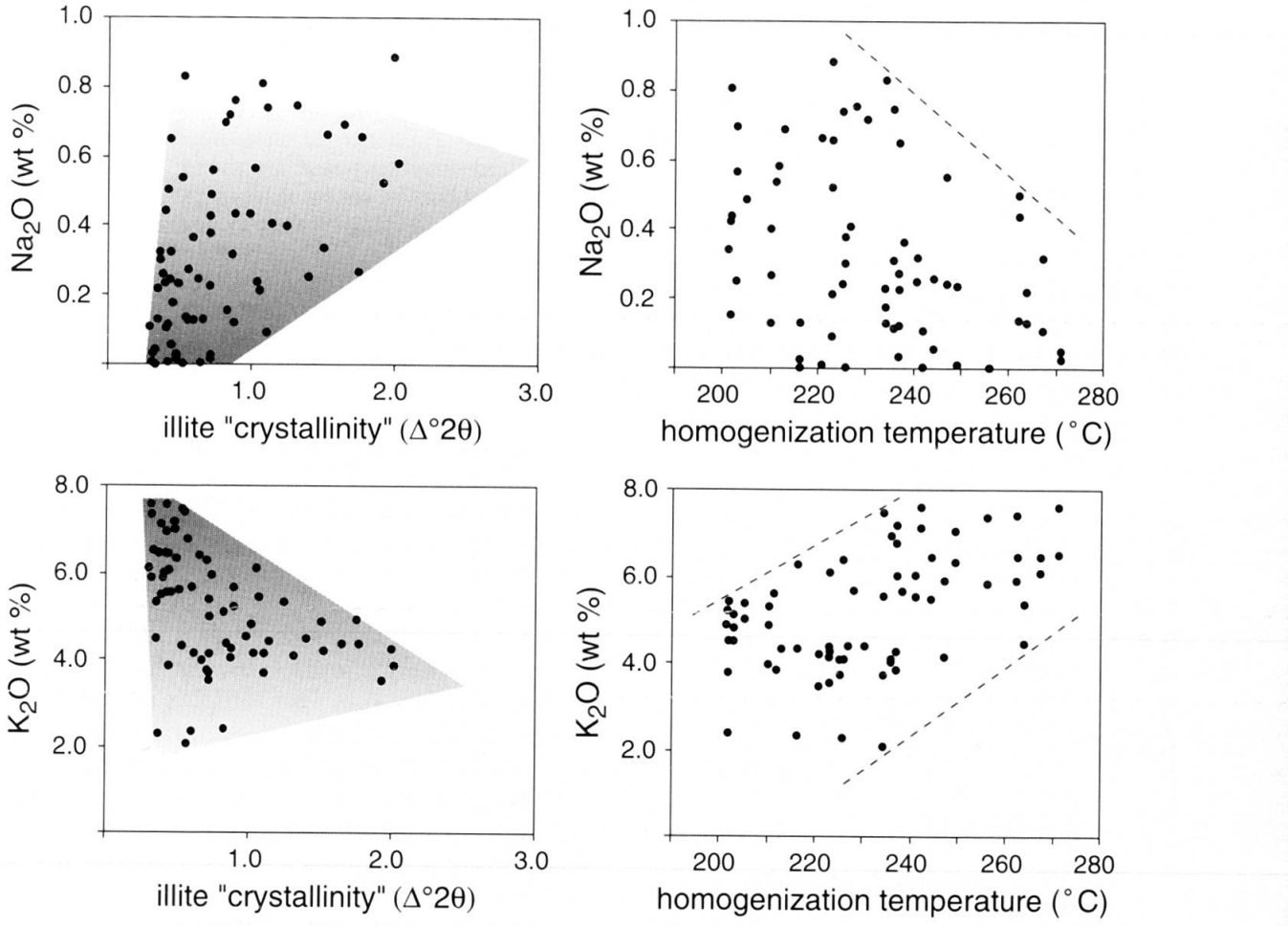

Fig. 6 Evolution of $Na_2O + K_2O$ with increasing illite "crystallinity" (left) and fluid inclusion homogenization temperature (right). At anchizonal conditions, illites become distinctly richer in K, but poorer in Na. Trends are underlined by shaded areas and dashed lines.

zonal illites have K_2O contents of up to 8 wt%; this corresponds to an interlayer occupation by K of ~75%. At the same metamorphic grade, the Na_2O content of the illite-smectite complex is reduced to less than 0.8 wt%. We conclude that no paragonite is produced, but the Na content in the illite phase decreases, while the K content increases with increasing temperature. In contrast to a simple reaction between smectite and illite (e.g. KYSER, 2000), the observed quantities of the K_2O take-up and Na_2O loss are not compatible with a simple exchange, as the K_2O gain is one order of magnitude larger than the Na_2O loss. The observed increase of K_2O with increasing temperature and the fact that the investigated smectites contain distinctly more Na_2O than the illites, requires a source of K outside of the clay fraction during the smectite to illite transition (BORGES et al., 1999; SON et al., 2001). A likely process is the decomposition of K-feldspar with increasing temperature. K-feldspar is not visible in the clay fraction but small amounts of this phase are commonly detected in bulk rock XRD patterns from the shales investigated. In this scenario, illite "crystallinity" would be controlled by an external process.

ILLITE "CRYSTALLINITY" AS A THERMOMETER?

From a simple plot of illite "crystallinity" versus temperature (Fig. 2) it is evident that the variation in the FWHM of the non-deconvoluted X-ray peak complex is markedly influenced by temperature, as well as by the amount of the smectitic phase (Fig. 4). Three samples shown in Fig. 8 illustrate a large scatter of illite "crystallinity" values

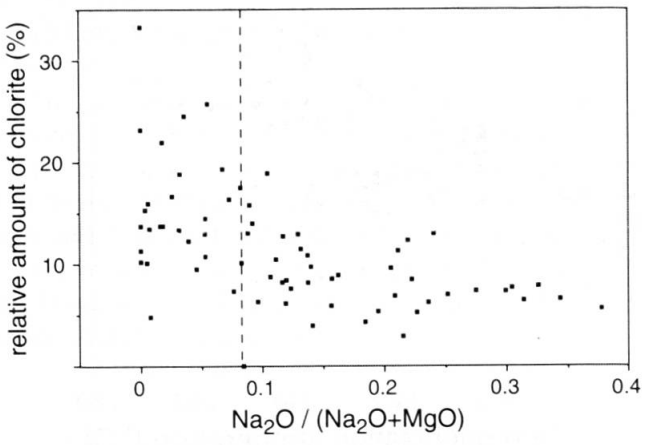

Fig. 7 Relationship between relative chlorite area (see text) and the $Na_2O/(Na_2O + MgO)$ ratio of the clay fraction. The vertical dashed line corresponds to the element ratio of 0.08 (see Fig. 5, diagrams at right).

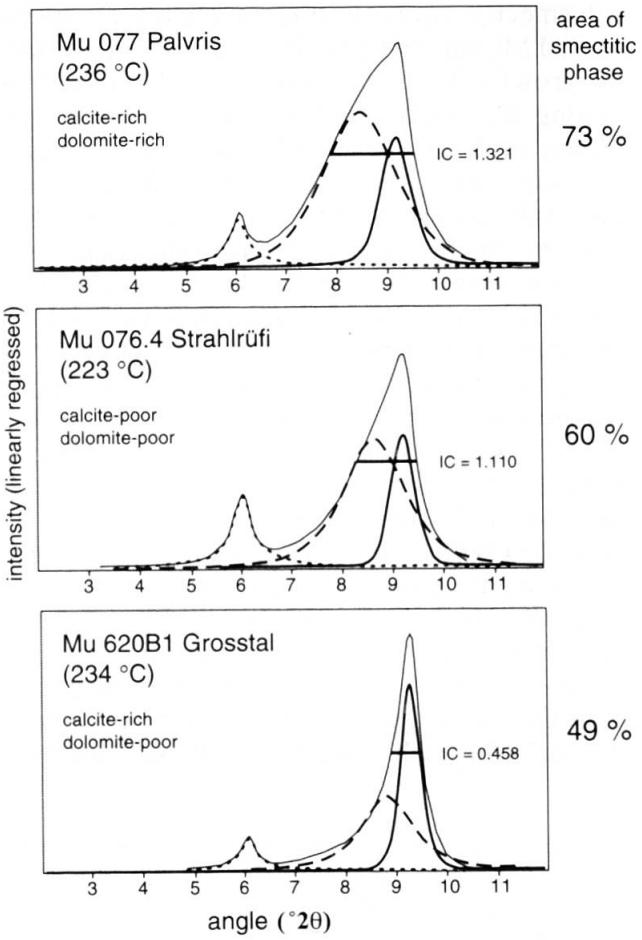

Fig. 8 Influence of smectite content (deconvolution fitted smectitic phase) on the illite "crystallinity" (horizontal bar) at constant temperature. The raw diffractogram is indicated by the enveloping thin line, the deconvoluted phases are an illitic-muscovitic phase (thick line), a smectitic phase (thick dashed line), and chlorite (thick dotted line). Note the variation in carbonate and dolomite content. The indicated IC values are given as $\Delta°2\theta$.

at nearly constant maximum temperature conditions (223–236 °C). At the same maximum temperature, the shape of the illite-smectitic peak complex changes from a weakly tailed peak with a position close to pure muscovite to a clearly bimodal distribution, with a saddle between the illite-smectite peak complex and the (001) chlorite peak. The example shown is further complicated by the fact that two samples are carbonate-rich, but dolomite poor, the sample with the largest illite "crystallinity", however, is dolomite-rich. As a consequence, the indicated trend is the result not only of different degrees of smectite formation during peak diagenesis, but also of early diagenesis and fluid composition. Similar observations can be made for samples of equal contents of smectitic phase and homogenization temperatures between 200 and 270 °C. A constant content in smectitic phase, but varying temperature leads

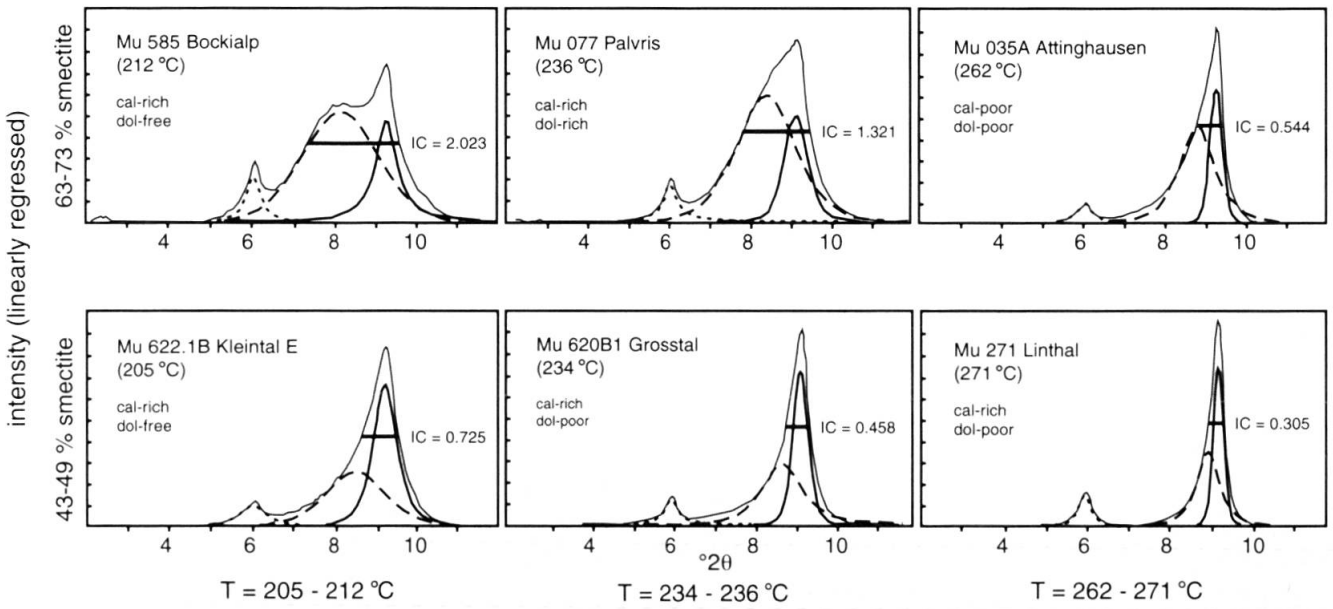

Fig. 9 Development of illite "crystallinity" with increasing fluid inclusion homogenization temperature at different contents of the smectitic phase (taken from deconvolution fitting). For the different stroke patterns, see Fig. 6. Note the different carbonate and dolomite contents at high smectitic phase content, but constant compositional parameters at low smectitic phase content.

to a variation in illite "crystallinity" by a factor 2 (for samples with low smectite contents) to 3 (for samples with high smectite contents) (Fig. 9). While the chosen suite of samples with high smectite contents is strongly variable in dolomite contents, the suite of low smectite samples are all carbonate-rich, but dolomite-poor. These observations raise some doubts about the reliability of the illite "crystallinity" parameter as a thermometer, as previously discussed by MULLIS et al. (1995). Consequently, the relationship between temperature and illite "crystallinity" would also have to include the bulk rock composition and the dolomite content as additional factors. Both of these were shown to be closely linked to the smectite content. A simple relationship between temperature, illite "crystallinity", and smectite content as the major influencing factor (Figs. 8, 9) has been evaluated by multiple linear regression. The correlation is given by:

$$T\ (°C) = 172 - 37*\ln\ (IC) + 0.77*(sm)$$

where IC is the measured illite "crystallinity" in $\Delta°2\theta$, and (sm) is the percentage of smectitic phase as obtained from deconvolution fitting with symmetric Pearson VII functions. The 1σ errors of the fitted parameters are: 172 ± 17 (=10% relative error), 37 ± 5 (13%), and 0.77 ± 0.27 (35%), and the reliablity of the statistical fitting is expressed by a regression factor r^2 of 0.51 and a reduced $\chi^2 = 15$ ($n = 71$). The errors illustrate that the content of smectitic phase is the least well constrained parameter in the mentioned relationship. The relation also underlines that illite "crystallinity" as an indicator of incipient metamorphism is a semi-quantitative measure at best. The same is true for "crystallinity" parameters derived from deconvolution, i.e. a "smectitic phase crystallinity" or "illitic-muscovitic phase crystallinity" (Fig 4).

TEMPERATURE OF THE DIAGENESIS-ANCHIZONE BOUNDARY

The diagenesis-anchizone boundary was defined by KÜBLER (1967) at an illite "crystallinity" value of 0.42 $\Delta°2\theta$. In our data set, diagenetic IC values are found up to (fluid inclusion derived) temperatures of 260 °C, while the first anchizonal value occurs at T = 225 °C (Fig. 10). The scatter in illite "crystallinity" is large below and strongly reduced above 240 °C. The diagenesis-anchizone boundary is interpreted to be around 240 ± 15 °C, i.e. at much higher temperatures than previously assumed (e.g. FREY, 1986). Based on the present data, a typical sample at 240 °C contains a calculated content of 40% of smectitic phase with a FWHM of 0.95 $\Delta°2\theta$ and a peak position at 10.5 Å (Fig. 4). The illitic-muscovitic peak has a FWHM of 0.35 $\Delta°2\theta$ and a d-value of 10.0 Å.

The obtained diagenesis-anchizone boundary is consistent with estimates based on other observations such as vitrinite reflectance (e.g. FERREIRO-MÄHLMANN, 1996) and mineral parageneses (e.g. RAHN et al., 1994). The presence of a peak

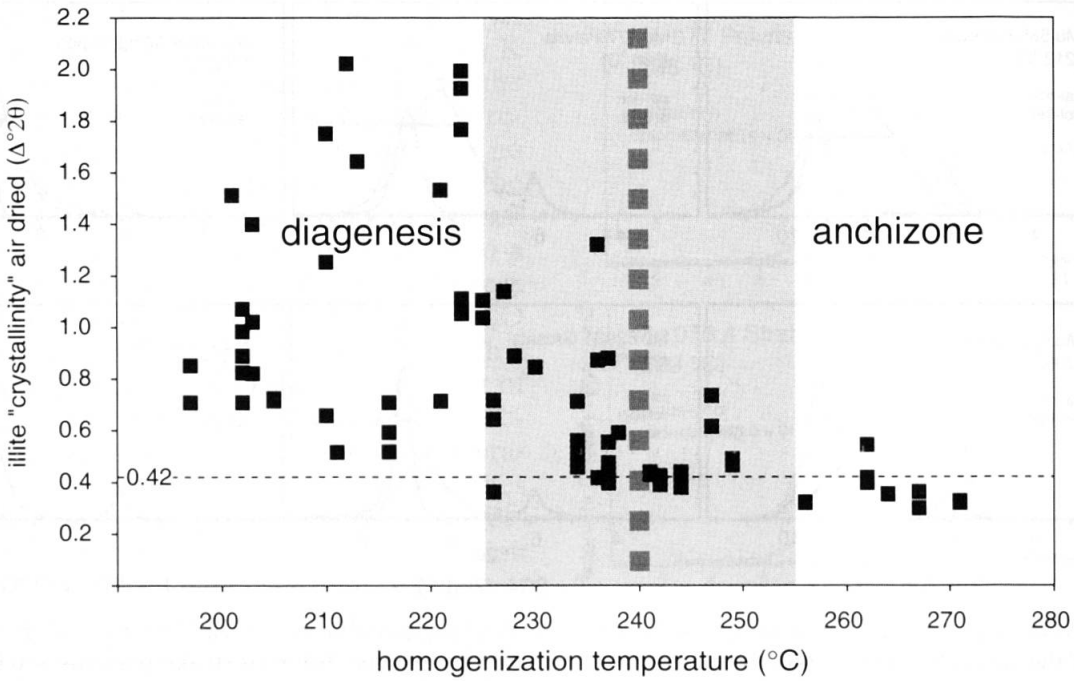

Fig. 10 Illite "crystallinity" versus fluid inclusion homogenization temperature in fibre quartz and the derived anchizone temperature boundary at $\Delta°2\theta = 0.42$ (KÜBLER et al. 1979). The uncertainty of the diagenesis-anchizone boundary temperature (± 15 °C) is indicated by the grey area.

corresponding to 40% of the smectitic phase cannot be translated directly to 40% of a swelling phase, which would be in contradiction to the initial definition of the anchizone, as a metamorphic level without any swelling component (KÜBLER, 1967). The comparison between air-dried and glycolated FWHM values of the unresolved illite-smectite complex at 10Å (Fig. 2) indicates that, with beginning of the anchizone at 240 °C, glycolation does not significantly change the FWHM values. The major reason for the calculated presence of 40% smectitic phase is probably the assumption of solely symmetric reflections used for deconvolution. MOORE and REYNOLDS (1989) showed that the asymmetry of the (001) illite peak is a function of crystallite size and hence of metamorphic grade. We submit that part of the calculated smectitic content may be an artefact.

The temperature of 240 °C obtained for the diagenesis-anchizone boundary should be tested in other terranes in order to ascertain whether it is generally applicable or typical only of a fast evolution as in the European Alps, with moderate pressure conditions, and a time span of approximately 30 million years between burial (defined e.g. by the age of the Taveyannaz event, RUFFINI et al., 1997) and final exhumation of the samples. Furthermore, the influence of the lithology on illite "crystallinity" (e.g. in BREITSCHMID, 1982) has to be evaluated in more detail.

Conclusions

The investigated samples from the external part of the Central Alps cover a range of maximum temperatures between 200 and 270 °C (based on fluid inclusion data). Illite "crystallinity" measurements and mathematical deconvolution procedures defining the FWHM and d-values of a smectitic and an illitic-muscovitic phase justify the following conlusions:

(a) Bulk rock composition (from shale to marly limestone) has a distinct influence on illite "crystallinity" values, by lowering peak widths by a factor of up to 2 in carbonate-rich samples (Fig. 3).

(b) Dolomite-rich samples with minor clay content can have very high illite "crystallinity" values. Rather than acting as a source of Mg for smectite formation, dolomite indicates early diagenetic high saline fluids, which lead to the formation of Na-bearing smectite in both carbonate- and clay-rich samples.

(c) The amount of smectitic phase (determined by deconvolution) shows a close relationship with the composition of the $< 2\ \mu$ fraction, notably its $Na_2O/(Na_2O + MgO)$ ratio, indicating that smectite has high Na contents.

(d) A correlation between the classic illite "crystallinity" parameter, the content of the smectitic phase, and temperature was used to test how reliable a thermometer illite "crystallinity" is. The accuracy of the derived thermometer turns out to

be restricted due to bulk rock variation and its influence on the smectite-illite transition.

(e) For the investigated external parts of the Central Alps, the comparison between illite "crystallinity" and fluid inclusion temperatures indicates that the boundary diagenesis-anchizone is located at a temperature of 240 ± 15 °C. At diagenetic conditions, illite "crystallinity" cannot be used as a temperature indicator, except for samples of well-defined lithologies of constant composition. Above 240 °C, across different lithologies, illite "crystallinity" values show considerably less scatter and serves as an approximate temperature indicator. The distinct increase in K_2O, parallel to a much smaller decrease in Na_2O, requires a K source outside the clay fraction.

Acknowledgements

Martin Frey and Bernard Kübler were the spiritual fathers for the present contribution. Thankfully we remember their stimulating and critical discussions in our future work. We like to thank M. Engi and L. Warr for their constructive reviews. Helpful contributions to data processing were provided by M. Sun and H. Wang. T. Heijboer helped with figure drawing. Financial support for this study was given by grants of the Swiss National Science Foundation to the first two authors (21-27.555.89 and 21-33868.92), and by travel grants to the authors by the University of Basel, the Freiwillige akademische Gesellschaft, Basel, and the Albert-Ludwigs-Universität Freiburg (to M. Rahn).

References

BAULUZ, B., PEACOR, D.R. and GONZALEZ-LOPEZ, J.M. (2000): Transmission electron microscopy study of illitization in pelites from the Iberian Range, Spain; layer-by-layer replacement? Clays and Clay Miner. 48, 374–384.

BORGES , J.B., MACK, D.M., HANAN, M.A. and TOTTEN, M.W. (1999): Clay-mineral diagenesis in the Louisiana Gulf Coast, how much K is needed for the smectite-illite transition. Abstracts with Programs. Geol. Soc. America 31, p. 160.

BREITSCHMID, A. (1982): Diagenese und schwache Metamorphose in den sedimentären Abfolgen der Zentralschweizer Alpen (Vierwaldstätter See, Urirotstock). Eclogae geol. Helv. 75, 331–380.

ERDELBROCK, K. (1994): Diagenese und schwache Metamorphose im Helvetikum der Ostschweiz (Inkohlung und Illit-"Kristallinität"). Unpubl. Ph.D. thesis, Univ. Aachen, 220 pp.

ESSENE, E.J. and PEACOR, D.R. (1995): Clay mineral thermometry – a critical perspective. Clays and Clay Miner. 43, 540–553.

FERREIRO-MÄHLMANN, R. (1994): Zur Bestimmung von Diagenesehöhe und beginnender Metamorphose – Temperaturgeschichte und Tektogenese des Austroalpins und Südpenninikums in Vorarlberg und Mittelbünden. Frankfurter geowissenschaftliche Arbeiten, Serie C, 14, 498 pp.

FERREIRO-MÄHLMANN, R. (1995): Das Diagenese-Metamorphose-Muster von Vitrinitreflexion und Illit-"Kristallinität" in Mittelbünden und im Oberhalbstein; Teil 1, Bezüge zur Stockwerktektonik. Schweiz. Mineral. Petrogr. Mitt. 75, 85–122.

FERREIRO-MÄHLMANN, R. (1996): Das Diagenese-Metamorphose-Muster von Vitrinitreflexion und Illit-"Kristallinität" in Mittelbünden und im Oberhalbstein; 2, Korrelation kohlenpetrographischer und mineralogischer Parameter. Schweiz. Mineral. Petrogr. Mitt. 76, 23–46.

FREY, M. (1986): Very low-grade metamorphism of the Alps – an introduction. Schweiz. Mineral. Petrogr. Mitt. 66, 13–27.

FREY, M. (1987): Very low-grade metamorphism of clastic sedimentary rocks. In: FREY, M. (ed.): Low temperature metamorphism. Blackie & Son, Glasgow. p. 9–58.

FREY, M., TEICHMÜLLER, M., TEICHMÜLLER, R., MULLIS, J., KUENZI, B., BREITSCHMID, A., GRUNER, U. and SCHWIZER, B. (1980): Very low-grade metamorphism in external parts of the Central Alps; illite crystallinity, coal rank and fluid inclusion data. Eclogae geol. Helv. 73, 173–203.

JABOYEDOFF, M., BUSSY, F., KÜBLER, B. and THÉLIN, P. (2001): Illite "crystallinity" revisited. Clays and Clay Miner. 49, 156–167.

KISCH, H. (1991): Illite crystallinity: recommendations on sample preparation, X-ray diffraction settings, and interlaboratory samples. J. Metamorphic Geol. 9, 665–670.

KÜBLER, B. (1967): La cristallinité de l'illite et les tones tout à fait supérieures du métamorphisme. In: Étages tectoniques, Colloque de Neuchâtel 1966, À la Baconnière, Neuchâtel, Suisse, 105–121.

KÜBLER, B., PITTION, J.-L., HEROUX, Y., CHAROLLAIS, J. et WEIDMANN, M. (1979): Sur le pouvoir réflecteur de la vitrinite dans quelques roches du Jura, de la Molasse et des Nappes préalpines, helvétiques et penniniques. Eclogae geol. Helv. 72, 347–373.

KYSER, K. (2000): Fluids and basin evolution. Short course Handbook 28. Mineral. Assoc. Canada, Ottawa, 262 pp.

LANSON, B. and CHAMPION, D. (1991): The I/ S-to-illite reaction in the late stage diagenesis. Am. J. Sci. 291, 473–506.

LANSON, B. and BESSON, G. (1992): Characterization of the end of smectite-to-illite transformation; decomposition of X-ray patterns. Clays and Clay Miner. 40, 40–52.

LANSON, B. and VELDE, B. (1992): Decomposition of X-ray diffraction patterns; a convenient way to describe complex I/S diagenetic evolution. Clays and Clay Miner. 40, 629–643.

MERRIMAN, R.J. and PEACOR, D.R. (1999): Very low-grade metapelites: mineralogy, microfabrics and measuring reaction progress. In: FREY, M. and ROBINSON, D. (eds): Low-Grade Metamorphism, Blackwell Science, Oxford, 10–60.

MOORE, D.M. and REYNOLDS, R.C. (1989): X-ray diffraction and identification of clay minerals. Oxford University Press, Oxford.

MULLIS, J. (1976): Das Wachstumsmilieu der Quarzkristalle im Val d'Illiez (Wallis, Schweiz). Schweiz. Mineral. Petrogr. Mitt. 52, 219–268.

MULLIS, J. (1979): The system methane-water as a geologic thermometer and barometer from the external part of the Central Alps. Bull. Minéral. 102, 526–536.

MULLIS, J. (1987): Fluid inclusion studies during very low-grade metamorphism. In: FREY, M. (ed.): Low temperature metamorphism. Blackie & Son, Glasgow. p. 162–199.

MULLIS, J. (1997): The application of fluid inclusions to fluid geochemistry and geothermobarometry in dia-

genetic and low-grade metamorphic rocks in the exernal parts of the Central Alps. XIV ECROFI European current Research on Fluid Inclusions, Nancy, France, July 1–4, 1997. M.C. Boiron and J. Pironon (eds): Abstract Volume, 224–225.

MULLIS, J., DUBESSY, J., POTY, B. and O'NEIL, J. (1994): Fluid regimes during late stages of a continental collision: Physical, chemical and stable isotope measurements of fluid inclusions in fissure quartz from a geotraverse through the Central Alps, Switzerland. Geochim. Cosmochim. Acta 58, 2239–2267.

MULLIS, J., RAHN, M., DE CAPITANI, C., STERN, W.B. and FREY, M. (1995): How good is illite "crystallinity" as a geothermometer? Abstract supplement 1, Terra nova 7, 128–129.

OVERSTOLZ, M. (2001): Diagenesis of Triassic Bunter Gas reservoirs in field "A" and surrounding fields, West Netherlands Basin. Unpubl. diploma thesis, Univ. of Basel, 50 pp.

POTY, B., LEROY, J. and JACHIMOWICZ, L. (1976): Un nouvel appareil pour la mesure des températures sous le microscope: l'installation de microthermométrie Chaixmeca. Bull. Minéral. 99, 182–186.

RAHN, M., MULLIS, J., ERDELBROCK, K. and FREY, M. (1994): Very low-grade metamorphism of the Taveyanne greywacke, Glarus Alps, Switzerland. J. Metamorphic Geol. 12, 625–641.

RAHN, M.K., MULLIS, J., ERDELBROCK, K. and FREY, M. (1995): Alpine metamorphism in the North Helvetic flysch of the Glarus Alps, Switzerland. Eclogae geol. Helv. 88, 157–178.

ROBINSON, D. and SANTANA DE ZAMORA, A. (1999): The smectite to chlorite transition in the Chipilapa geothermal system, El Salvador. Am. Mineralogist 84, 607–619.

RUFFINI, R., POLINO, R., CALLEGHARI, E., HUNZIKER, J.C. and PFEIFFER, H.-R. (1997): Volcanic clast-rich turbidites of the Taveyanne sandstones from the Thônes syncline (Savoie, France): records for a Tertiary postcollisional volcanism. Schweiz. Mineral. Petrogr. Mitt. 77, 161–174.

SON, B.K., YOSHIMURA, T. and FUKASAWA, H. (2001): Diagenesis of dioctahedral and trioctahedral smectites from alternating beds in Miocene to Pleistocene rocks of the Niigata Basin, Japan. Clays and Clay Miner. 49, 333–346.

STERN, W.B., MULLIS, J., RAHN, M. and FREY, M. (1991): Deconvolution of the first "illite" basal reflection. Schweiz. Mineral. Petrogr. Mitt. 71, 453–462.

SWEENEY, J.J. and BURNAM, A.K. (1991): Evaluation of a simple model of vitrinite reflectance based on chemical kinetics. Am. Assoc. Petrol. Geol. Bull. 74, 1559–1570.

TUCKER, M.E. and WRIGHT, V.P. (1990): Carbonate Sedimentology. Blackwell Sci. Publ., Oxford.

WANG, H., FREY, M. and STERN, W.B. (1996): Diagenesis and metamorphism of clay minerals in the Helvetic Alps of eastern Switzerland. Clays and Clay Miner. 44, 96–112.

Manuscript received February 7, 2002; revision accepted June 11, 2002.
Editorial handling: M. Engi